Disordered Berezinskii-Kosterlitz-Thouless transition and superinsulation

S. Sankar, V. M. Vinokur, and V. Tripathi

Phys. Rev. B **97**, 020507 — Published 22 January 2018

DOI: 10.1103/PhysRevB.97.020507

Disordered BKT transition and superinsulation

S. Sankar,[1] V. M. Vinokur,[2] and V. Tripathi[1]

[1] *Department of Theoretical Physics, Tata Institute of Fundamental Research, Homi Bhabha Road, Navy Nagar, Mumbai 400005, India*

[2] *Materials Science Division, Argonne National Laboratory, 9700 S. Cass. Ave, Lemont, IL 60437, USA.*

We investigate the critical Berezinskii-Kosterlitz-Thouless (BKT) behavior of disordered two-dimensional Josephson-junction arrays (JJA) on the insulating side of the superconductor-insulator transition (SIT) taking into account the effect of hitherto ignored residual random dipole moments of the superconducting grains. We show that for weak Josephson coupling the model is equivalent to a Coulomb gas subjected to a disorder potential with logarithmic correlations. We demonstrate that strong enough disorder transforms the BKT divergence of the correlation length, $\xi_{\rm BKT} \propto \exp(\text{const}/\sqrt{T-T_{\rm BKT}})$, characterizing the average distance between the unbound topological excitations of the opposite signs, into a more singular Vogel-Fulcher-Tamman (VFT) behavior, $\xi_{\rm VFT} \propto \exp[\text{const}/(T-T_{\rm BKT})]$, which is viewed a hallmark of a glass transitions in glass-forming materials. We further show that the VFT criticality is a precursor of the transition into a nonergodic superinsulating state, while the BKT critical behavior implies freezing into an ergodic confined BKT state. Our finding sheds the light on the yet unresolved problem of the origin of the VFT criticality.

I. INTRODUCTION

More than 40 years ago, celebrated works by Berezinskii, Kosterlitz, and Thouless (BKT) introduced the idea of topological phase transitions where pairs of bound topological vortex-like excitations unbind at the critical temperature.[1–4] Soon after, the fundamental importance of BKT theory for understanding two-dimensional (2D) superconductivity was demonstrated[5–8] in films and planar Josephson junction arrays (JJA), where superconductivity was described as a low-temperature BKT phase with vortices and antivortices bound in vortex dipoles (see for a review A. M. Goldman in Ref. [9] and also Ref. [10]). Above the BKT transition temperature, $T_{\rm BKT}$, the proliferation of low-energy vortices breaks down the global phase coherence, and the 2D superconducting systems fall into the resistive state.

Diamantini *et al.* introduced the concept of a superinsulating state in the framework of the gauge theory of Josephson junction arrays (JJA)[11] as a realization of the Cooper pair-vortex duality,[12–14] and later it was proposed in Ref. [15] that the superinsulator is a low-temperature charge-BKT state. The zero temperature superconductor-insulator transition (SIT) then corresponds to the mutual termination of charge- and vortex BKT transitions at the self-dual point.[13,16,17] The self-dual point separates a superconducting state that harbors Cooper pair condensate and pinned vortices from a superinsulating state where Bose condensation of vortices inhibits charge transport.[14,15,17] The dual picture leads to similar vortex and Cooper pair dynamics on either side of the SIT.[13] The divergence of the dielectric constant near the SIT in strongly disordered superconductor thin films which in turn leads to 2D logarithmic Coulomb interactions between the Cooper pairs over appreciably macroscopic scales[15] provides a material platform for the realization of charge BKT physics. This conjecture was found to comply with the experimental data on TiN films[16] and earlier experimental benchmarks of the superinsulating state.[18,19] The dielectric constant diverging on approach to the SIT from the insulating side was recently observed in thin NbTiN films.[20]

The BKT critical behavior[4] of the sheet resistance upon approaching the *vortex* BKT transition temperature, $T_{\rm VBKT}$, from above, $R \propto \exp[-b/\sqrt{1-T/T_{\rm VBKT}}]$, has been reported in numerous works (see A. M. Goldman in Ref. 9). Recent observations of the *charge* BKT critical behavior $R \propto \exp[b/\sqrt{1-T/T_{\rm CBKT}}]$[16,20] is consistent with the dual BKT physics of the SIT.[13] Recent measurements[21] of the temperature dependence of the sheet resistance of InO_x thin films on the insulating side in the vicinity of a field-tuned SIT reported, however, a surprising observation of much more singular, the so called Vogel-Fulcher-Tammann (VFT)-like critical behavior of the resistance, $R(T) \sim \exp[\text{const}/(T-T_{\rm VFT})]$. This VFT dependence is viewed as a standard critical behavior in glass-forming materials, but its origin remains a puzzle in spite of the decades-long search, see Ref. [22] for a review. At the same time, an earlier suggestion made by Anderson[23] that the origin of the VFT may also lie in logarithmic interactions between topological defects in the glass-forming materials, makes it appealing to revisit the theory of disordered superconductor films and to examine whether the VFT criticality may arise in the framework of the BKT physics. We will show that this is indeed the case.

We investigate here the nature of BKT criticality in strongly disordered superconductor thin films in the framework of the *disordered* JJA model that hosts both vortex and charge BKT transitions. Depending on the ratio of the characteristic Josephson coupling energy $E_{\rm J}$ and the Coulomb charging energy of a single junction, $E_{\rm C}$, one obtains either a superconducting phase for $E_{\rm J} > E_{\rm C}$, or insulating phase for $E_{\rm J} < E_{\rm C}$.[13] For concreteness and also to connect with the recent experiment[21], we focus here on the insulating regime. Apart from the well-studied effect of nucleating Cooper pair islands,[24] we argue that potential disorder is also a source of quenched

random dipole moments. We show that such disorder in the dipole moments, if sufficiently strong, turns the standard BKT critical behavior of conductivity

$$\sigma(T) \sim e^{-\mathrm{const}/\sqrt{T-T_{\mathrm{BKT}}}} \tag{1}$$

into the more singular VFT criticality

$$\sigma(T) \sim e^{-\mathrm{const}/(T-T_{\mathrm{VFT}})}\,. \tag{2}$$

The difference of critical behaviors comes from poorer electrostatic screening (in the VFT case) due to the freezing of charge dipole excitations that is known to occur[25] in the absence of interactions of the dipole-dipole kind once disorder strength exceeds a critical value. This critical strength is determined by the ratio of temperature and Coulomb interaction scales. Based on this consideration, we posit that the VFT and BKT phases respectively correspond to nonergodic and ergodic regimes of the superinsulator. The strong disorder criterion is $\eta > T/2E_{\mathrm{C}}$, where dimensionless parameter η defines the strength of disorder via the correlation function of the coarse-grained random dipole potential, $\langle (V(\mathbf{r}) - V(\mathbf{r}'))^2\rangle \approx 4\eta E_{\mathrm{C}}^2 \ln(|\mathbf{r}-\mathbf{r}'|/R)$. We construct the disorder vs. temperature phase diagram of the superinsulator transition, and this, along with the critical behaviors given by Eqs. (1) and (2) and the phase diagram of the BKT critical region constitute the main result of our work.

II. JJA MODEL AND DISORDERED COULOMB GAS DESCRIPTION

We consider a homogeneously disordered two-dimensional superconductor on the insulating side of the SIT. Coarse-graining over the size of the Cooper pairs, we approximate the disorder background charge distribution $\rho(\mathbf{r})$ as a Gaussian white noise correlation function, $\langle(\rho(\mathbf{r})-\bar\rho)(\rho(\mathbf{r}')-\bar\rho)\rangle = n_d\delta(\mathbf{r}-\mathbf{r}')$, where the average background charge density, $e\bar\rho$, equals the average charge density of the Cooper pairs, and n_d is the variance of the coarse-grained background charge distribution. The angular brackets stand for averaging over disorder. Near the SIT the dielectric constant diverges $\kappa \gg 1$, see Ref. 16 and references therein, and in a film of thickness t, the Coulomb interaction between two charges has logarithmic separation r dependence as $\ln(\Lambda/r)$ over distances $t < r < \Lambda$, where $\Lambda \simeq \kappa t$ is an electrostatic screening length[16,26]. At distances beyond Λ the interaction falls off as $1/r$. The system is customarily viewed as a lateral JJA comprising superconducting droplets coupled by Josephson links[16]. The droplets nucleate at deep potential fluctuations resulting from intrinsic quenched charge disorder of the host. Near the SIT, the size of the droplets is expected to be of order of the superconducting coherence length and in any case exceed the characteristic localization length of single particles in the disordered potential[24,27,28]. In the JJA, the effective dielectric constant and, accordingly, the crossover length is expressed via the characteristic capacitances[13]. We will address the situation $\Lambda \gtrsim L$ so that the interactions between the charges is logarithmic.

The excess charge on a droplet interacts with the charge distribution of other droplets. The leading contribution to the energy is provided by the electric 'monopoles', the single excess charges $n_{\mathbf{i}}$ on the other droplets, $-\sum_{\mathbf{i}\neq\mathbf{j}} E_{\mathrm{C}} n_{\mathbf{i}} n_{\mathbf{j}} \ln|(\mathbf{r_i}-\mathbf{r_j})/a|$, where a is a microscopic length scale (the size of the droplet), $E_{\mathrm{C}} = q^2/2C$ is the characteristic energy for creation of a CP dipole ($q = 2e$) across neighboring droplets and C is the inter-droplet capacitance[13]. The next order contribution comes from the dipole moments of the grains, $\mathbf{P_i}$, which yield the random potential energy

$$V_{\mathbf{i}} = \sum_j \frac{q}{2\pi C}\frac{\mathbf{P}_j\cdot\mathbf{r}_{ij}}{r_{ij}^2}. \tag{3}$$

Using $\langle\mathbf{P}\rangle = 0$, we derive, analogously to[29], that the dipole-induced random potential is logarithmically correlated:

$$\langle (V(\mathbf{r}) - V(\mathbf{r}'))^2\rangle \approx 4\eta E_{\mathrm{C}}^2 \ln(|\mathbf{r}-\mathbf{r}'|/R)\,, \tag{4}$$

where $\eta = \pi\langle P^2\rangle/q^2R^2$, R is the typical radius of a grain and $\langle P^2\rangle \propto n_d$.

The effective action for JJA comprises both, the charge and phase degrees of freedom. Trading off the phase degrees of freedom for vortex variables via the Villain transformation[13] gives the well-known Fazio-Schön action

$$S[n,v] = \int_0^\beta d\tau \sum_{\mathbf{i,j}} \Big(E_{\mathrm{C}} n_{\mathbf{i}} U_{\mathbf{ij}} n_{\mathbf{j}} + E_{\mathrm{J}} v_{\mathbf{i}} U_{\mathbf{ij}} v_{\mathbf{j}} + \iota n_{\mathbf{i}} \Theta_{\mathbf{ij}} \partial_\tau v_{\mathbf{j}} + \frac{1}{2E_{\mathrm{J}}} \partial_\tau n_{\mathbf{i}} U_{\mathbf{ij}} \partial_\tau n_{\mathbf{j}} \Big) + \sum_i V_i n_{\mathbf{i}}, \tag{5}$$

where $v_{\mathbf{i}}$ are the integer-valued vortex degrees of freedom, defined on the dual lattice, $\Theta_{\mathbf{ij}} = \arctan\left(\frac{y_i-y_j}{x_i-x_j}\right)$ and $U_{ij} = -\ln|\mathbf{r}_i - \mathbf{r}_j|$. In the insulating state where $E_{\mathrm{J}} \ll E_{\mathrm{C}}$, E_{J} being the typical strength of the Josephson coupling, we can treat the integer valued vortex fields as continous fields and integrate them out to obtain the effective charge action as

$$S_e[n] = \int_0^\beta d\tau \sum_{\mathbf{i,j}} U_{\mathbf{ij}} \left(\frac{1}{E_{\mathrm{J}}} \partial_\tau n_{\mathbf{i}} \partial_\tau n_{\mathbf{j}} + E_{\mathrm{C}} n_{\mathbf{i}} n_{\mathbf{j}} \right) + \sum_i V_{\mathbf{i}} n_{\mathbf{i}}\,. \tag{6}$$

Hereafter we neglect the temporal fluctuations as they are irrelevant at low energies and do not alter the nature of the phase transition governed by the interplay of the long-range Coulomb interaction and disorder correlations. The parameters in the model are thus the temperature T, Coulomb energy scale E_{C} and the effective disorder strength η.

III. RESULTS FROM SCALING ANALYSIS

A scaling analysis of our classical 2D Coulomb gas Hamiltonian in Eq. (6) proceeds through analyzing the disorder averaged real-space Kosterlitz renormalization group (RG) equations. This RG analysis has been performed by Carpentier and Le Doussal,[30] and we discuss the results relevant to our study in this section.

To deal with quenched disorder, one introduces replicas and performs the average over disorder to obtain the disorder-averaged replica Coloumb gas Hamiltonian (with m replicas),

$$\beta H^{(m)} = \sum_{i\neq j} K_{ab} n_i^a \ln\left(\frac{|\mathbf{r}_i - \mathbf{r}_j|}{a_0}\right) n_j^b + \sum_i \ln Y[\mathbf{n}_i]. \tag{7}$$

Here the superscripts on the charges refer to the replica index, $Y[\mathbf{n}] = \exp(-n^a \gamma K_{ab} n^b)$ is the fugacity, $K_{ab} = \beta E_{\rm C}\delta_{ab} - \eta\beta^2 E_{\rm C}^2$ is the effective coupling, and a_0 is of the order of the lattice constant and serves as a short length cutoff as we go over to the continuum description. Disorder averaging mixes different replicas and the extent of this mixing, which is controlled by disorder strength η, has a qualitative effect on the phase diagram and critical behavior.

To $O(Y[\mathbf{n}]^2)$, one obtains the following RG flow equations for the effective coupling and fugacity as we rescale from $a_0(\ell)$ to $a_0(\ell + d\ell) = a_0 e^{d\ell}$ (thus, $a_0 e^{\ell}$ is the spatial scale over which short wave-length excitations have been integrated out by RG):

$$\partial_\ell (K_\ell^{-1})_{ab} = 2\pi^2 \sum_{\mathbf{n}\neq 0} n^a n^b Y[\mathbf{n}] Y[-\mathbf{n}], \tag{8}$$

$$\partial_\ell Y[\mathbf{n}\neq 0] = (2 - n^a K_{ab} n^b) Y[\mathbf{n}] + \sum_{\mathbf{n}'\neq 0,\mathbf{n}} \pi Y[\mathbf{n}'] Y[\mathbf{n}-\mathbf{n}']. \tag{9}$$

Equation (8) comes from the annihilation of dipoles of opposite vector charges in the annulus $a_0 < |r_i - r_j| < a_0 e^{d\ell}$. Simple rescaling gives the first part of Eq. (9). The second part, a new contribution that is absent in the disorder-free case, comes from the possibility of "fusion" of unit charges in two different replicas upon coarse graining. Here fusion refers to the possibility of combining two vector charges with the ± 1 charges occuring in different replica indices.

The analysis of the above RG equations has been performed in Ref. [30]. The phase boundary between the superinsulating (XY phase) and normal insulating (disordered) phases is given by

$$2 - \frac{E_{\rm C}}{T} + \frac{\eta E_{\rm C}^2}{T^2} = 0 \text{ for } T > T_g = E_{\rm C}\sqrt{\frac{\eta}{2}}; \tag{10}$$

$$\eta = \eta_c = \frac{1}{8} \text{ for } T \leq T_g, \tag{11}$$

where $E_{\rm C}$ and η stand for the renormalized quantities at $\ell = \infty$.

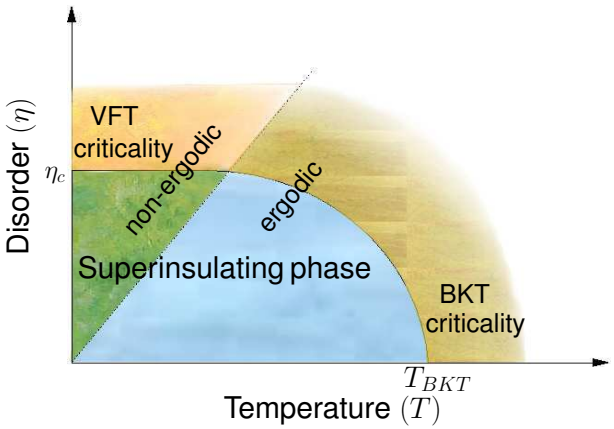

Figure 1. A sketch of the phase diagram of the superinsulating state and critical behaviours of a two-dimensional Josephson-junction disordered array in disorder-temperaure coordinates. Disorder being considered is the quenched random dipole moments of the grains. In the superinsulating phase, the probability of single charge excitations is zero. The transition to the conducting state occurs via the proliferation of the single charge excitations generated either thermally or by disorder. The former leads to the BKT criticality, given by Eq. (1), while the latter results in VFT behavior of Eq. (2). The dotted line $\eta = T/2E_{\rm C}$, separates the nonergodic region (shaded green), where the charge dipoles freeze (their free energy becomes independent of temperature), from the ergodic region (shaded blue) where a finite entropy is associated with the charge dipoles which can appear anywhere. Likewise, the VFT critical region is nonergodic and conducting, while the BKT critical region is ergodic and conducting.

Two distinct critical behaviors are identified on approach to the charge BKT transition. Near the phase boundary at small degrees of disorder, the correlation length exhibits the usual BKT criticality

$$\xi \sim e^{1/\sqrt{b/[(T/T_{\rm BKT})-1]}},\ (T - T_{\rm BKT})/E_{\rm C} \ll 1\,, \tag{12}$$

where, $T_{\rm BKT} = E_{\rm C}/2$ is the critical temperature of the charge-BKT transition [13] and b is a numerical constant of order unity. For finite but small disorder η, the dependence of $T_{\rm BKT}$ on η can be obtained from the solution of Eq. (10). Near the disorder-controlled phase boundary, the correlation length is

$$\xi \sim e^{1/(\eta-\eta_c)},\ T/E_{\rm C} \ll 1,\ \eta - \eta_c \ll 1\,, \tag{13}$$

where $\eta_c = 1/8$ is the critical disorder strength at low temperatures for the transition.

IV. ERGODIC AND NONERGODIC REGIMES

To understand the physics underlying these two critical scenarios, we look at a dilute gas of charge dipoles subjected to disorder and neglect the dipole-dipole interations. Here, the distinct critical scenarios correspond to

the system freezing into either the ergodic, at low disorder, or into the nonergodic, at strong disorder, respectively, superinsulating states as shown in the phase diagram in disorder-temperature coordinates in the Fig. 1. The dotted line $\eta^*(T) = T/2E_{\rm C}$, marks the onset of freezing of isolated charge dipoles [25] where freezing means that the free energy of dipole excitations loses an explicit temperature dependence. To see this, consider a dilute gas of dipoles, where the inter-dipole distance D far exceeds the typical dipole size R. In this dilute limit, we focus on a region of linear size D containing a single dipole. The energy of this dipole is

$$E_d \sim 2(\ln Y + E_C \ln(R/a_0)) + (V^{(+)}(\mathbf{r}) - V^{(-)}(\mathbf{r}')), \tag{14}$$

where $V^{(\pm)}$ refer to the respective potential energies of the positive and negative charge constituting the dipole, $|\mathbf{r}-\mathbf{r}'| = R$. The first term is a uniform part and the latter term is a random contribution. Although $V^{(+)}$ and $V^{(-)}$ individually have long-range correlations, their difference is short-range correlated beyond the scale R. The variance of this random potential difference is easily seen to be $\Delta = 4\eta E_C^2 \ln(r/a_0)$. Thus we effectively have a single particle (the dipole) subjected to a Gaussian white noise random potential with variance Δ. Factoring out the constant part of the energy, we construct the partition function for the random energies of different charge configurations,

$$Z = \sum_N \exp[-\beta E_d^i], \tag{15}$$

where i labels the charge configuration, $N \sim (D/a_0)^2(R/a_0)^2$ is the total number of configurations. This random energy model has been extensively studied in the literature.[31] The free energy is known to have the following form,

$$F = -c(T,s)\ln N + O(\ln\ln N), \tag{16}$$

where,

$$c(T,s) = \begin{cases} T + s/2T & \text{for} T > T_g(s) \\ \sqrt{2s} & \text{for} T < T_g(s) \end{cases} \tag{17}$$

Here $s = \Delta/\ln N$ and $T_g(s) = \sqrt{s/2}$. Then for our case, we have,

$$s = \frac{2\eta E_C^2 \ln(R/a)}{\ln(R/a_0) + \ln(D/a_0)}. \tag{18}$$

The free energy is given by,

$$F_d(D,T) \sim 2(\ln Y + E_C \ln(R/a_0)) - 2c(T,s)\ln\left(\frac{DR}{a_0^2}\right) \tag{19}$$

The freezing now takes place at $T^* = T_g(s)$. The typical inter-dipole distance D can be determined from the condition, $F_d(D,T) = 0$. The D thus determined will then initially increase as T decreases and then lock to a value D^* as $T < T^*$. Thus T^* is obtained by self consistently solving the equation,

$$T^* = T_g(s^*), \tag{20}$$

with s^* given by (18) by putting $D = D^*$. The solution is then given by, $T^* = 2\eta E_C$.

In the ergodic phase the dipoles can appear anywhere and thus assume the most efficient – for screening – configuration. In the nonergodic phase, the dipoles are frozen, as they emerge mostly due to fluctuations in the random quenched potential, and hence may not provide an efficient screening as compared to the one due to thermally generated dipoles. This then leads to the more singular VFT-like critical behavior. In the presence of dipole-dipole interactions, it remains an open question as to whether the above transition remains a true one or becomes a crossover.

V. CHARGE TRANSPORT IN THE CRITICAL REGION

The experimentally measurable quantity is conductivity, $\sigma \simeq \mu_c n_c$, where μ_c is the charge mobility and $n_c \sim 1/\xi^2$ is the density of free charges in the critical regime [7]. Then Eq. (12) leads us to our result in Eq. (1), i.e., the vanishing of conductivity in accordance with the BKT law.

We next address the conductivity in the strong disorder case described by Eq. (13). In Sec. III, the disorder strength was treated as a temperature independent parameter. However in our description of the effective JJ model (see Sec. II), η in general depends on the temperature. Physically, increasing the temperature increaes the ionization of the dopants. We assume an activated temperature dependence $n_d(T) = n_d(0) + N_d e^{-E_d/T}$, where E_d is the characteristic dopant-carrier binding energy for dopant levels near the conduction or valence bands. The temperature dependence of n_d imparts a temperature dependence to the disorder strength, η. Let T_c be the temperature at which $\eta(T_c) = \eta_c$. Expanding $n_d(T)$ in the vicinity of T_c, $n_d(T) \approx n_d(T_c)[1 + (T - T_c)(E_d/T_c^2)]$, we recover the VFT law for conductivity near the *disorder*-driven transition with $T_{\rm VFT} = T_c$ and constant $= 2T_c^2/(E_d\eta(T_c))$. Note that this result is obtained under the condition $T_c < E_{\rm C}/2$, for otherwise the condition for the thermally-driven BKT transition is satisfied first with the increasing temperature and one obtains the BKT behavior of Eq. (1) as expected for the weak disorder case. Comparing VFT and BKT results one concludes that the transition from the VFT to the BKT behavior occurs at $\eta(T_{\rm BKT}) = \eta_{\rm c}$. Different critical behaviors in the strongly and weakly disordered regimes implies the existence of two distinct phases of the superinsulator.

VI. DISCUSSION

In summary, we have shown that in strongly disordered superconductor thin films, a logarithmically interacting 2D charge Coulomb gas may be realized in the vicinity of the SIT, where the dielectric constant tends to diverge. Apart from the well-known formation of superconducting islands, we proposed that quenched disorder also induces quenched random dipole moments of the charge distribution of the superconducting islands, which in turn, is the source of long-range (logarithmically) correlated potential fluctuations acting on the charge excitations. We also showed that the strength of the long-range correlated disorder increases with temperature. At low temperatures, a charge BKT (superinsulator) phase is realized, characterized by a vanishing conductivity. Increasing the temperature ultimately results in a BKT transition to a normal insulator phase. We showed that in the critical normal region, the conductivity continuously vanishes in accordance with two different laws - the usual BKT law for small disorder strengths, and a more singular VFT law for strong disorder strengths. We posit that these two distinct critical behaviors are manifestations respectively of ergodic and non-ergodic regimes of the superinsulator phase. The transition from the ergodic to nonergodic regimes is associated with the freezing of single charge dipole excitations.

By observing the critical behavior experimentally, we can understand if the system undergoes a transition to the ergodic or nonergodic superinsulating state. Based on the existing data, we suggest that disordered superconducting TiN and NbTiN films [15,16,20] exhibit transition into the ergodic phase of the superinsulator, while the VFT criticality reported in InO films [21] suggests nonergodic behavior.

An analogous situation may also arise in the context of the superconducting transition in these systems in the presence of a finite magnetic field. Here, random Aharanov-Bohm phases associated with Cooper pair hopping lead to a (logarithmically) long-range correlated disorder for the vortex Coulomb gas.[29,30] The crossover length separating 2D and 3D Coulomb regimes is now the Pearl screening length, $\lambda_{\rm P} = \lambda^2/t$, where λ is the standard London penetration depth and t is the thickness of the superconducting film. Vortices tend to appear in regions of small local superfluid stiffness, and analogously to the residual charge dipoles discussed above, one now has residual vortex dipoles oriented along random directions. Since the (vortex) disorder parameter η is proportional to the density of randomly oriented vortex dipoles, increasing the temperature leads to the excitation of more dipoles in the weak-link regions thereby increasing η. Proceeding with the analysis we followed for the superinsulator phase, we arrive at essentially the same phase diagram and critical behavior for the superconductor phase. Owing to the vortex-charge duality, here the resistivity vanishes in accordance with either the BKT or VFT law upon approaching the superconducting phase boundary. A signature of the nonergodic superconducting phase would be the resistivity critically vanishing according to the VFT law. Instead of tuning the temperature, one can also tune an external (perpendicular) magnetic field to control the disorder parameter η (see Ref. 28). The same critical scaling now appears in the magnetic field dependence of resistance near the field tuned superconductor-insulator transition.

In Ref. 21, the authors propose that their finite temperature insulator transition could be a manifestation of the many-body localization (MBL) transition.[32,33] The rationale behind this suggestion is that the Cooper pairs are only weakly coupled to the phonons, which is one of the prerequisites for observing an MBL transition. In what follows, we compare and contranst our picture with those obtained in the MBL framework. The critical behavior of $\sigma(T)$ on approaching the MBL transition proposed in Ref.[32] is identical to our result for the ergodic BKT regime, while a recent result for conductivity in the vicinity of a many-body localized phase [34] resembles our nonergodic BKT behavior of Eq. (13).

A key difference is that in our picture, the zero conductivity phase is the result of long-range Coulomb interactions and turning up the disorder ultimately takes us out of this phase, while, in the MBL picture, the zero conductivity state is underpinned by disorder, and, Coulomb interactions provide the means to delocalize the charges. Historically, MBL studies have focused on the case with the short range interactions, but the recently proposed extension of MBL to a model with long-range interactions[35] challenges the earlier understanding that MBL does not occur for long range interactions.[36]. We further note that while the MBL phase is essentially nonergodic, our superinsulating phase is ergodic for $T > 2\eta E_{\rm C}$, and non-ergodic for $T < 2\eta E_{\rm C}$. In the nonergodic region, the transition from the superinsulating phase to the conducting phase is reminiscent of the transition to nonergodic conducting regime derived in the MBL framework.[37] The comparison of BKT and MBL pictures is summarized in Table I .

Acknowledgments– The authors are delighted to thank P. LeDoussal and R. Nandkishore for illuminating discussions. The work is supported by the U.S. Department of Energy, Office of Science, Materials Sciences and Engineering Division (V.M.V.) and by Department of Science and Technology, Govt. of India, through a Swarnajayanti grant (no. DST/SJF/PSA-0212012-13) (V.T.).

[1] V. L. Berezinskii, Zh. Eksp. Theor. Fiz. (Sov. Phys.– JETP, **32**, 493-500 (1970)) **59**, 907 (1970).

[2] V. L. Berezinskii, Zh. Eksp. Theor. Fiz. (Sov. Phys.– JETP,

Property	Quantum many-body localization	2D disordered Coulomb gas
Role of disorder and interactions	Disorder underpins MBL, interactions provide a mechanism for delocalization.	Long-range (logarithmic) interactions responsible for superinsulation. Disorder facilitates transition from superinsulator to normal insulator.
Nature of interaction	Finite temperature insulator has been demonstrated for short range interactions. However a recent study claims that the MBL considerations can be extended to long range interactions also.[35]	Logarithmic Coulomb interaction germane to finite temperature insulator. Further, VFT scaling for $\sigma(T)$ requires logarithmically correlated disorder.
Mechanism	$\sigma(T) = 0$ if the gap in the spectrum of many-particle bath excitations exceeds the corresponding inelastic scattering rate.[32,33] Finite σ due to thermal activation above mobility edge not possible as mobility edge diverges with system volume.[33]	(a) Low disorder ($\eta \ll \eta_c$): Transition from superinsulator phase $\sigma(T) = 0$ occurs when long-range Coulomb interaction gets screened by thermally generated low-energy charge dipole excitations. (b) High disorder ($\eta > \eta_c$): Transition occurs due to seeding of low-energy single charge excitations due to deep potential fluctuations.
Erogodicity	MBL phase is nonergodic. Recent work[37] suggests existence of a nonergodic delocalized phase near the MBL phase, and also that the transition between the nonergodic and ergodic delocalized phases resembles the classical glass transition.	Phase diagram has both ergodic and nonergodic regions with respect to the occurence of charge dipoles. Dilute gas of dipoles freezes[25] for $T/E_c < \eta$. Transition from XY to conducting phase can take place in both the ergodic and nonergodic regions resulting in KT-like or VF-like scaling respectively for $\sigma(T)$.
Cayley tree structure	Transition temperature and critical behaviour are obtained by an approximate mapping of the problem to an Anderson model in Fock space with a Cayley tree structure.	Scaling equation for charge fugacity in the disordered model can be recast in the form of the KPP equation[30] in relevant variables. The KPP equation arises naturally in studies of directed polymers on the Cayley tree.[38]

Table I. Comparison of two different theoretical routes to superinsulating behaviour based on (i) quantum many body localization and (ii) 2D disordered Coulomb gas (proposed in this paper).

34, 610-616 (1971)) **61**, 1144 (1971).

[3] J. M. Kosterlitz and D. J. Thouless, J. Phys. C: Solid State Phys. **5**, L124 (1972).

[4] J. M. Kosterlitz and D. J. Thouless, J. Phys. C: Solid State Phys. **6**, 1181 (1973).

[5] D. R. Nelson and J. M. Kosterlitz, Phys. Rev. Lett. **39**, 1201 (1977).

[6] M. R. Beasley, J. E. Mooij, and T. P. Orlando, Phys. Rev. Lett. **42**, 1165 (1979).

[7] B. I. Halperin and D. R. Nelson, J. Low Temp. Phys. **36**, 599 (1979).

[8] C. J. Lobb, D. W. Abraham, and M. Tinkham, Phys. Rev. B **27**, 150 (1983).

[9] E. José, J V, *40 Years of Berezinskii-Kosterlitz-Thouless Theory* (World Scientific, 2013).

[10] T. I. Baturina, S. V. Postolova, A. Y. Mironov, A. Glatz, M. R. Baklanov, and V. M. Vinokur, EPL **97**, 17012 (2012).

[11] M. C. Diamantini, P. Sodano, and C. A. Trugenberger, Nuclear Physics B **474**, 641 (1996).

[12] M. P. A. Fisher, Physical Review Letters **65**, 923 (1990).

[13] R. Fazio and G. Schön, Physical Review B **43**, 5307 (1991).

[14] A. Krämer and S. Doniach, Physical Review Letters **81**, 3523 (1998).

[15] V. M. Vinokur, T. I. Baturina, M. V. Fistul, A. Y. Mironov, M. R. Baklanov, and C. Strunk, Nature **452**, 613 (2008).

[16] T. I. Baturina and V. M. Vinokur, Annals of Physics **331**, 236 (2013).

[17] M. C. Diamantini, C. A. Trugenberger, I. Lukyanchuk, and V. M. Vinokur, arXiv:1710.10575 (2017).

[18] G. Sambandamurthy, L. W. Engel, A. Johansson, and D. Shahar, Physical Review Letters **92**, 107005 (2004).

[19] T. I. Baturina, A. Y. Mironov, V. M. Vinokur, M. R. Baklanov, and C. Strunk, Physical Review Letters **99**, 257003 (2007).

[20] A. Y. Mironov, D. M. Silevitch, T. Proslier, S. V. Postolova, M. V. Burdastyh, A. K. Gutakovskii, T. F. Rosenbaum, V. M. Vinokur, and T. I. Baturina, arXiv:1707.09679 (2017).

[21] M. Ovadia, D. Kalok, I. Tamir, S. Mitra, B. Sacepe, and D. Shahar, Scientific reports **5**, Article:13503 (2015).

[22] J. Rault, Journal of Non-Crystalline Solids **271**, 177 (2000).

[23] P. W. Anderson, II condensed matter Les Houches, 159 (1979).

[24] G. M. Falco, T. Nattermann, and V. L. Pokrovsky, Physical Review B **80**, 104515 (2009).

[25] L.-H. Tang, Physical Review B **54**, 3350 (1996).

[26] N. Rytova, Vestnik MSU (in Russian) **3**, 30 (1967).

[27] A. I. Larkin and V. M. Vinokur, Physical review letters **75**, 4666 (1995).

[28] S. Sankar and V. Tripathi, Phys. Rev. B **94**, 054520 (2016).

[29] A. Petković, V. M. Vinokur, and T. Nattermann, Physical Review B **80**, 212504 (2009).

[30] D. Carpentier and P. Le Doussal, Nuclear Physics B **588**, 565 (2000).

[31] B. Derrida, Phys. Rev. B **24**, 2613 (1981).

[32] I. V. Gornyi, A. D. Mirlin, and D. G. Polyakov, Phys. Rev. Lett. **95**, 2006603 (2005).

[33] D. M. Basko, I. L. Aleiner, and B. L. Altshuler, Annals of Physics **321**, 1126 (2006).

[34] S. Gopalakrishnan and R. Nandkishore, Phys. Rev. B **90**, 224203 (2012).
[35] Nandkishore, Rahul M., and S. L. Sondhi, Phys. Rev. X **7**, 041021 (2017).
[36] L. Fleishman and P. W. Anderson, Physical Review B **21**, 2366 (1980).
[37] B. Altshuler, E. Cuevas, L. Ioffe, and V. Kravtsov, Phys. Rev. Lett. **117**, 156601 (2016).
[38] B. Derrida and H. Spohn, Journal of Statistical Physics **51**, 817 (1988).